3
Investigation of cellular and molecular pathways of innate immunity in response to amorphous nanosilica particles on different cell types

3.1 Abstract

Nucleotide-binding domain, leucine-rich repeat-containing proteins (NLRs) are a family of pattern recognition receptors involved in major innate immune defense mechanisms to maintain immune surveillance. NLRs identify an array of danger-associated molecular patterns (DAMPs), pathogen-associated molecular patterns (PAMPs) and irritants such as silica [Saïd-Sadier and Ojcius, 2012]. Some NLRs form a multiprotein complex also called as an inflammasome that consists of an NLR, procaspase-1, and ASC (Apoptosis-associated speck-like protein containing a C-terminal caspase recruitment domain [CARD]) [Guo *et al.*, 2015]. Exposure to amorphous nano-silica is considered largely non-toxic and has been proposed to have widespread applications in targeted drug delivery, bio-nanopesticides, and cosmetics. I utilized amorphous silica nanoparticles of size 12nm and 22nm to study distinct size and time-dependent pathways of cytotoxicity on human bronchoalveolar epithelial and endothelial. Cytotoxic effects of amorphous silica nanoparticles were measured by MTT cytotoxicity assay, showing endothelial cells are most susceptible to cell death among the three cell populations. Immunofluorescence and confocal microscopy were utilized to identify the formation and spatial localization of ASC specks in different lung cell populations following nanosilica treatment. We also investigated the size-dependent distinct cell death pathways involved with 12nm and 22nm silica nanoparticles. Cells treated with 12nm nanosilica showed characteristic necrotic cell death while 22nm nanosilica suggested apoptotic cell death, which was confirmed and quantified by Annexin V and propidium iodide staining by flow cytometry. Our results suggest size and the time-dependent difference in cytotoxicity, spatial localization of ASC, and cell death pathways in endothelial and epithelial after nanosilica treatment.

3.2 Introduction

Nanoparticles are defined as particles having a diameter less than 100nm and specific surface area of > 60 m^2/cm^3. The surface area of the nanoparticles further defines the critical parameters of the nanoparticles, such as chemical reactivity and toxicity. Along with the size and surface area of the nanoparticles, there are other properties such as shape, agglomeration state, crystal structure, porosity and surface chemistry, which also define the properties of nanoparticles [Kreyling *et al.*, 2010; Oberdörster *et al.*, 2005]. Silica is the common name of silicon dioxide (SiO_2) [Napierska *et al.*, 2010]. Silica occurs in two major forms, amorphous and crystalline. Silica nanoparticles have different physio-chemical properties as compared to the corresponding bulk forms as the smaller size has more surface-to-volume ratio and surface reactivity. The biological effects of the silica nanoparticles are quite different from the micro-scale particles. Considering these properties, nanosilica particles are widely used in different industries such as cosmetics, food, and agriculture. They are also used for different biomedical purposes, such as drug delivery, dental fillers, and implants [Tang and Cheng, 2013]. The disorders related to crystalline nanosilica exposure such as silicosis, tuberculosis, chronic pulmonary obstructive disorder (COPD), lung cancer, and rheumatoid arthritis has been extensively studied [Leung *et al.*, 2012]. However, amorphous nanosilica owing to its stability is widely considered not to be harmful. The studies addressing the toxicity of amorphous nanosilica particles are limited.

Nucleotide-binding domain, leucine-rich repeat-containing (NBD-LRR) proteins (NLRs) are pattern recognition receptors (PRRs) that recognize evolutionarily conserved sequences present in pathogens referred to as PAMPs (Pathogen associated molecular patterns) and sterile activators derived from inside the cells called as DAMPs (Danger associated molecular patterns). Irritants such as titanium oxide, silica, asbestos, and metal alloys also elicit an innate immune response via NLRs [Ruiz *et al.*, 2017, Baron, 2015 #1578, Ferko, 2018 #1579, Chow, 2012 #1580]. NLRs are generally composed of three separate domains; N-terminus, pyrin domain, caspase recruitment domain, or a baculovirus inhibitory repeat domain, central nucleotide-binding domain (NBD) and C-terminus leucine-rich repeats (LRRs). Upon exposure to PAMPs, DAMPs or irritants some NLRs form a multiprotein complex called inflammasome that consists of an NLR, procaspase-1, and ASC (Apoptosis-associated speck-like protein containing a CARD). Inflammasome initiates auto-cleavage of procaspase-1 into active form caspase-1, which further cleaves pro- IL-1β and pro-IL-18 into their mature form, IL-1β, and IL-18. ASC is an adaptor protein. There are well established cellular changes downstream of silica exposure that leads to the activation of NLRP3 inflammasome. Reactive oxygen species (ROS) production, lysosomal rupture, potassium ion efflux, and mitochondrial disturbances are among the few cellular changes which lead to the activation of NLRP3 upon silica exposure [Hornung *et al.*, 2009, Sayan, 2016 #1581].

There are several properties that affect the biocompatibility of silica nanoparticles and even subtle differences in the physio-chemical properties, size and shape can lead to major differences in the cytotoxicity and mode of action in the concerned model system[Auffan *et al.*, 2009]. Within the nanoscale (1-100nm) also the particles may act differently as the nanoparticles below the size of 30nm are considered to have high energy on the surface leading to instability. Smaller the particle higher the surface-to-volume ratio, that leads to the increased area for the binding proteins. Although crystalline silica-induced inflammatory responses have been well studied, there are limited studies considering the hazardous effects of amorphous silica nanoparticles[Yazdi *et al.*, 2010, Cassel, 2008 #5]. In this study, I have investigated the role of the intracellular adaptor protein, ASC in the presence of amorphous silica nanoparticles on human bronchoalveolar epithelial, and endothelial cell lines. I have also evaluated the size-dependent

differences in cytotoxicity, spatial localization of ASC, and cellular uptake of silica nanoparticles in endothelial cells. In the present study, we are utilizing two amorphous silica nanoparticles with two different sizes, i.e., 12nm and 22nm, to study their effect on cell cytotoxicity in human bronchoalveolar epithelial cells, endothelial cells and fibroblast cells.

3.3 Materials and Methods

3.3.1 Characterization of Amorphous Silica Nanoparticles

The silica nanoparticles used in this study are Ludox® colloidal silica nanoparticles TM-40 (420786) and HS-40 (420816) available from Sigma. These are monodispersed amorphous silica nanoparticles suspended in water. For Transmission Electron Microscopy, 10µL solution of Ludox® silica was deposited on carbon-coated copper grids. The samples were imaged using FEI Tecnai™ transmission electron microscope (T 20 S-twin, FEI) at the Materials Research Centre facility of Malaviya National Institute of Technology (MNIT), Jaipur. For cell culture experiments, silica nanoparticles were diluted, re-suspended in freshly prepared DMEM serum-free medium and vortexed just before use.

3.3.2 Cell culture

Human endothelial cell line HUVEC were obtained from Himedia (CL002) and grown on HiEndoXL™ endothelial cell expansion medium (Himedia, AL517). A-549 human lung carcinoma cell line was obtained from (Sigma-Aldrich, cat. no: 86012804). A-549 cells and BV-2 mouse microglial cell line were grown in Dulbecco's modified eagle medium (DMEM), (Himedia, AL007S) with 10% Fetal bovine serum (Himedia, RM10432) and 1% antibiotic antimycotic solution (Sigma-Aldrich, A5955). Cell lines were cultured as per company instructions in humidified CO_2 incubators. To stimulate inflammation, cells were pre-stimulated with Lipopolysaccharide overnight (0.5µg/mL, Sigma, L4391). -For phagocytosis inhibition, cells were pre-treated with 10µM cytochalasin-D for 20 minutes (Sigma, T6025).

3.3.3 MTT Assay

After exposure to silica nanoparticles, the cell cytotoxicity caused was assessed by the MTT assay. Nanosilica-containing media was removed carefully from the microplate. 100µl of fresh serum-free media and 10µl of MTT solution (M2128, Sigma) was added to each well. The plate was kept in an incubator (Model-170S, Eppendorf) at 37^0C with 5% CO_2 in the dark for 3 hours. After incubation, 100µl of acid/alcohol solution was added to each well. Absorbance was measured at 570nm using multi-mode microplate reader (Synergy H1 Hybrid, Biotek Instruments Inc).

3.3.4 Annexin V/ PI staining of cells

Cell death was analyzed using FITC Annexin V/ Dead Cell apoptosis kit (Invitrogen: V13242) according to manufacturers' instructions. Samples were analyzed using FACS Aria- III flow cytometer (BD Biosciences), and acquired data were further analyzed using FlowJo-Win64_10.1r5 software.

3.3.5 Bradford assay for protein estimation

For protein extraction from cultured cells, 0.25×10^6 cells were lysed in 0.25 ml RIPA buffer by rotating cell at 4°C for 20 minutes, followed by centrifugation at 13000rpm for 20 minutes. The supernatants were used for further analyses. Protein concentrations are determined using a coomassie (Bradford) protein assay. Absorbance was measured at 595nm using multi-mode microplate reader (Synergy H1 Hybrid, Biotek Instruments Inc).

3.3.6 Confocal Microscopy

Fluorescence confocal images were taken from Zeiss LSM 780 Laser Scanning Microscope at Bio-Organic Division, BARC, Mumbai with a 63X objective. 10^5 cells were grown in two-chamber slides and incubated overnight. The cells were treated with silica nanoparticles (200µg/ml) and cytochalasin–D (10µM). Treated cells were immunolabeled with anti-ASC/TMS-1 rabbit monoclonal antibody (Cell signaling Technology cat no: 13833S), and Alexa Fluor 594 goat anti-rabbit secondary antibody (Life technologies) and nuclei were counterstained by DAPI (Sigma). Zen 2011 software was used to analyze the images.

3.3.7 Scanning electron microscopy

Samples were prepared by centrifuging 20ml of nanosilica particles at 15000 rpm for 30 minutes. Nanosilica particles were spin-coated on the silicon wafer (width= 0.5mm, Resistivity = 0.1 ~ 1 ohm-cm, SSP (Single side polished), orientation <100> crystal structure) at 1000 rpm. The samples were then charged on the sputtering unit with Au-Pd target for about 6 minutes. The images were taken on the ZEISS EVO® MA and LS EVO 18(special edition) at 200nm and magnification of 67.37KX (supplemental data).

3.3.8 Transmission electron microscopy of the cells

Cells were treated with HS40 and TM40. After centrifugation, fixation of the treated cells was carried out using 2.5% glutaraldehyde and washed with PBS. This was followed by fixation of 1% Osmium tetroxide. Then, the cells were subjected to dehydration with a graded series of alcohol, then embedding was performed using an embedding kit, DER 332-732 (EMS, USA) and kept for polymerization for 48 hours. The resultant resin blocks were subjected to ultrathin sectioning using an ultra-microtome (Leica Ultracut UCT, Germany). 60-70 nm ultrathin section was transferred on the Formvar and carbon-coated copper grids (EMS, USA) of 300 mesh size. The grids were stained with Uranyl acetate and lead citrate solutions. The sections were visualized under Phillips TEM CM 200 at SAIF-IIT Bombay.

3.3.9 Caspase-1 activity assay

BV-2 cells were grown in chamber slides with 5 X 10^4 cells per well. After nanosilica treatment of BV-2 cells, the media was removed, and 50µM Ac-WEHD-amc (Sigma, A0216) substrate was added. Cells were incubated for 1 hour at 37°C under 5% CO2. 1µl of 1mg/ml propidium iodide (Life Technologies, V13242) was added for 5 minutes for staining the necrotic cells. The cells were fixed, mounted, and imaged using a Leica fluorescence microscope. For the fluorimetry experiment, 10 µg of the untreated, LPS treated and nanosilica treated BV-2 cells protein was added with 200 µl CFS buffer (10 mM HEPES, pH 7.4, 220 mM mannitol, 68 mM sucrose, 2 mM NaCl, 2.5 mM KH2PO4, 0.5 mM EGTA, 2 mM MgCl2, 0.5 mM sodium pyruvate, 0.5 mM L-glutamine, and 10 mM DTT) to each well of the 96 well plate. 50µM of Ac-WEHD-amc (Sigma, A0216) substrate was added per well. Caspase-1 activity was measured for 90 minutes at 1-min intervals by fluorimetry (excitation at 360 nm and emission at 480 nm) using multi-mode microplate reader.

3.4 Results and Discussion

3.4.1 12nm and 22nm nanosilica were different in surface morphology

The nanosilica particles were first characterized by scanning electron microscopy (Figure 3.1), but due to the limitation with the resolution of the microscope, we were limited to characterization of larger silica nanoparticles (22nm).

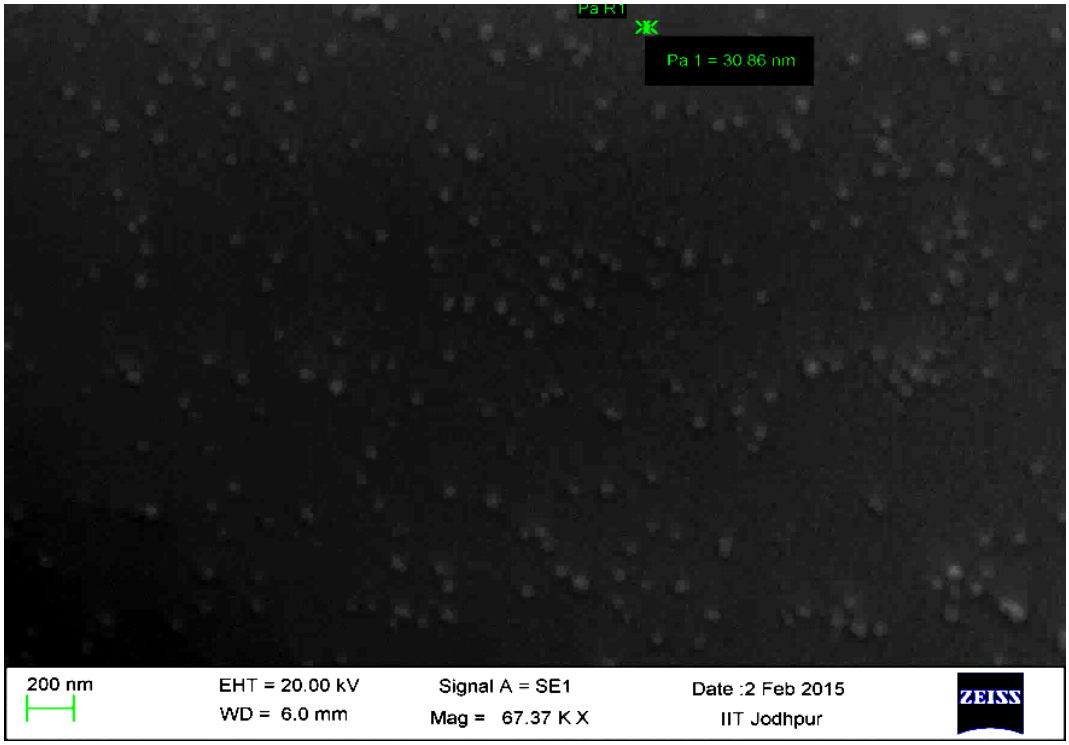

Figure **3.1**: Characterization of large silica nanoparticles (22nm) by scanning electron microscopy (SEM): The Ludox® silica particles TM-40(~22nm) were spin-coated on the silicon wafer (width= 0.5mm, Resistivity = 0.1 ~ 1 ohm-cm, SSP (Single side polished), orientation : <100> crystal structure) at 1000 rpm. The samples were then charged on the sputtering unit with Au-Pd target for about 6 minutes. The images were taken on the ZEISS EVO® MA and LS EVO 18(special edition) at 200nm and magnification of 67.37KX

Silica nanoparticles were further analyzed by transmission electron microscopy by Dr. Nidhi Sharma (Figure 3.2). The higher resolution of the transmission electron microscope allowed us to characterize both the 22nm and 12nm silica nanoparticles(3.2a-b); 22nm silica nanoparticles were round and smooth on the surface while the 12nm silica nanoparticles showed rough surface morphology (3.2 c-d).

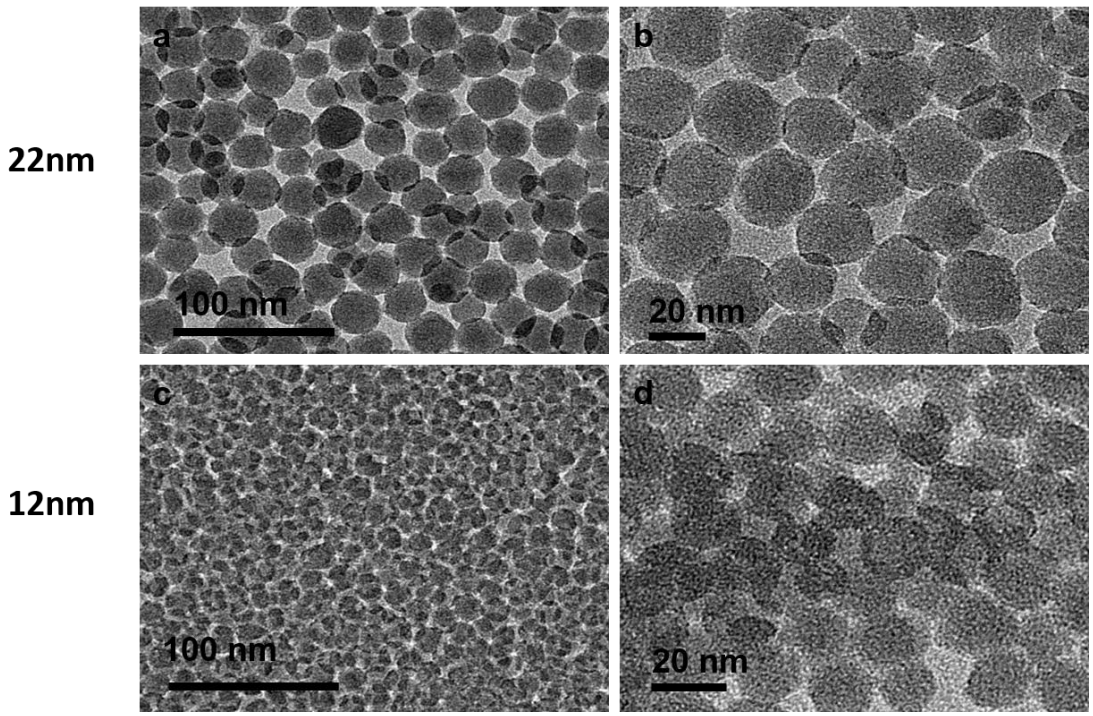

Figure 3.2: Characterization of amorphous silica nanoparticles by transmission electron microscopy 22nm nanosilica (a-b) and 12nm nanosilica (c-d).

The specifications of the particles are given in Table 1, which shows that the smaller silica nanoparticles (12nm) have a larger surface area as compared to larger silica nanoparticles (22nm).

Silica nanoparticles	**TM-40**	**HS-40**
Size	~22nm	~12nm
Surface area	~140 m^2/g	~220 m^2/g
Density	1.3 g/mL at 25 °C	1.3 g/mL at 25 °C
Concentration (percent by weight)	40 wt. % suspension in H_2O	40 wt. % suspension in H_2O
Concentration(mg/ml)	520.29	520.29

Table 3.1: Specifications of Amorphous nanosilica. The silica nanoparticles used in this study are ludox® colloidal silica nanoparticles TM-40, 22nm (Sigma) and HS-40, 12nm (Sigma). These are monodisperse amorphous silica nanoparticles suspended in water.

3.4.2 12 and 22nm silica nanoparticles elicit differential cell death response

For the purpose of the study, we have used three different cell lines, which are representative of the lung cell population, i.e., bronchoalveolar epithelial, endothelial, and fibroblast. The dose-dependent and time-dependent studies were previously conducted in my laboratory in fibroblast and epithelial cell lines. I was responsible for establishing the effect of silica nanoparticles in the endothelial cell line, Human umbilical vein endothelial cells (HUVEC). MTT assay was performed to quantify the silica nanoparticle-induced cell cytotoxicity in HUVEC. The 3-(4,5-dimethylthiazol-2-yl)-2,5-diphenyltetrazolium bromide(MTT) assay is cell viability assay. MTT is converted into insoluble formazan catalyzed by mitochondrial succinate dehydrogenase in metabolically active cells. HUVEC cells, when exposed to different concentrations of silica nanoparticles (100, 200, and 400µg/ml) for 1 hour, showed a concentration-dependent cell death (Figure3.3a-b). The silica nanoparticles dependent cell death was quantified both in the presence and absence of lipopolysaccharide (LPS) to stimulate the effects of preexisting inflammation (Figure3 c-d). LPS acts as a priming signal for the expression of pro-IL-1β and pro-IL-18 [Dinarello, 1998; Kaspar and Gehrke, 1994]. Pro-IL-1β and pro- IL-18 are not constitutively expressed inside cells, and transcriptional induction is achieved by NF-κβ pathway activation. LPS detection by TLR-4 is one of the common mechanisms of activation of NF-κβ pathway and consequent release of pro-IL-1β and pro-IL-18.

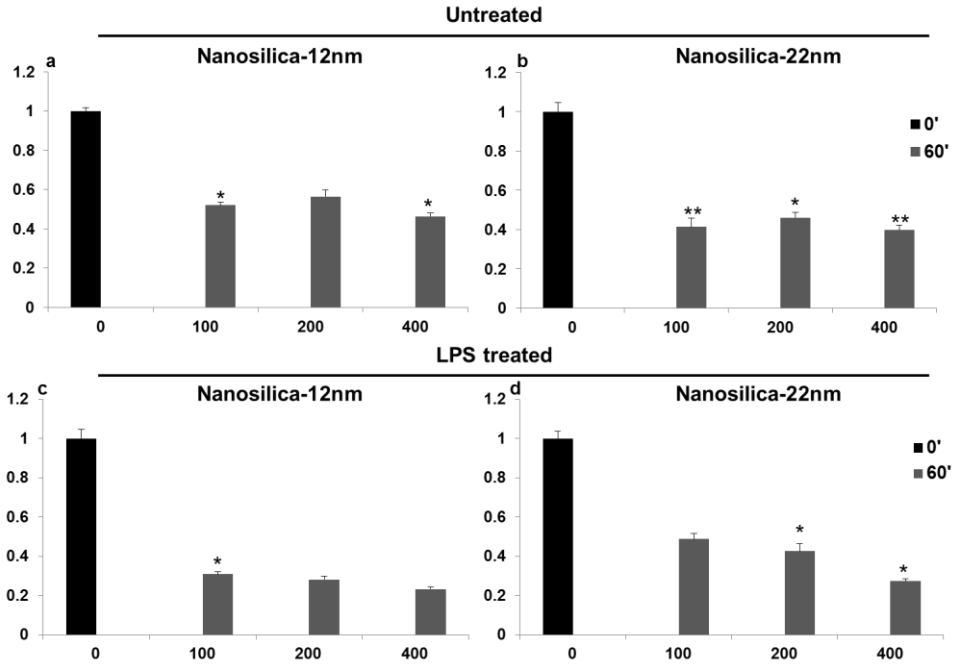

Figure 3.3 (a-d): MTT Assay for assessment of cell viability following nanosilica exposure. Endothelial cells were left untreated or treated with bacterial lipopolysaccharide (LPS, 0.5µg/ml) to simulate inflammation. Endothelial cells 0, 100, 200, and 400µg/ml 12nm and 22nm nanosilica exposure for 0 and 60 minutes were utilized. Each experiment had internal duplicates. Error bars indicate SEM. *p <0.05, **p<0.005, ***p<0.0005. Details of all p values for this figure are part of the supplemental data.

LPS treated endothelial cells did not induce a significant difference in the cytotoxicity. Endothelial cells were highly susceptible to nanosilica-induced cell death as compared to epithelial and endothelial cell lines (data not shown).

3.4.3 Larger silica nanoparticles shows a phagocytosis dependent cytotoxicity

Cytochalasin D is a cell-permeable fungal toxin, which inhibits actin polymerization by binding with high affinity to growing ends of actin nuclei and filaments (F-actin), and preventing the addition of monomers (G-actin)[Brenner and Korn, 1979; Casella *et al.*, 1981]. 12nm nanosilica could induce cytotoxicity in endothelial cells even after cytochalasin D treatment (Figure 3.4 a-d). Although the cytochalasin D treated 22nm endothelial cells showed lesser cytotoxicity as compared to the 12nm silica nanoparticles treated endothelial cells. This experiment led to the conclusion that the smaller silica nanoparticles are engulfed independent of phagocytosis, while larger silica nanoparticles are internalized by phagocytosis dependent and independent pathways in endothelial cells.

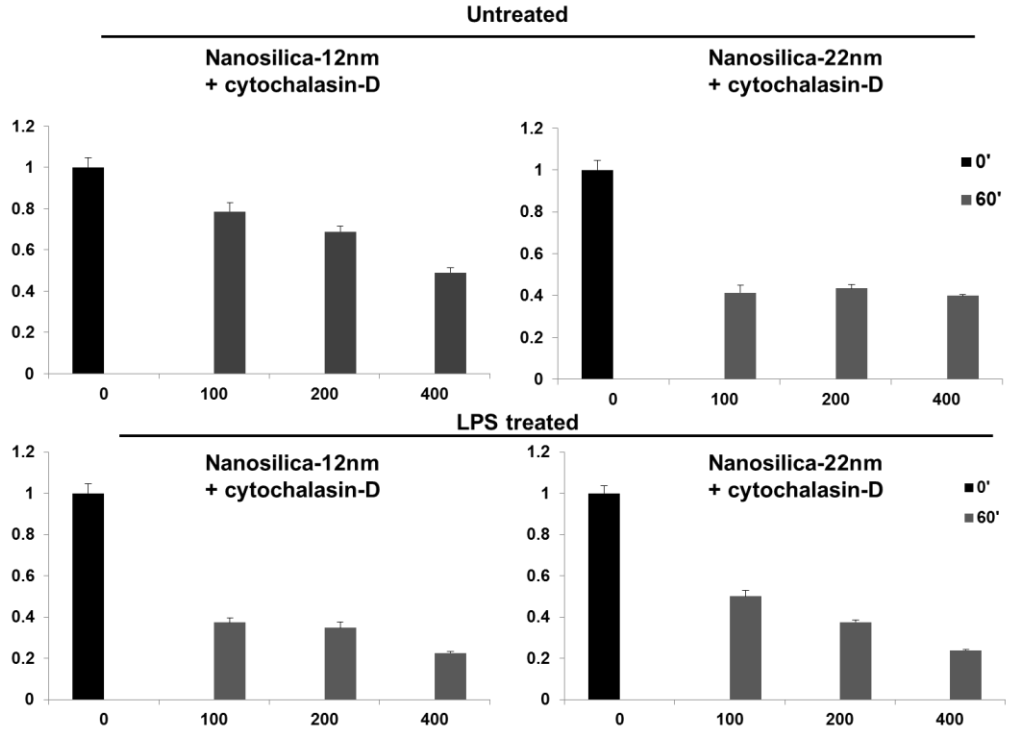

Figure 3.4 a-d: MTT assay for the assessment of cell death in the presence of Endothelial cells were left untreated (w/o LPS) or treated with LPS (0.5ug/ml) followed by cytochalasin–D (cyto-D) treatment (10μM, 20 minutes) prior to silica nanoparticles exposure (HS40 = 12nm, TM40= 22nm, 200μg/ml, 60 minutes) (3d). n=3 for each experiment. Each experiment had internal duplicates. Error bars indicate SEM.*p <0.05, **p<0.005, ***p<0.0005. Details of all p values for this figure are part of the supplemental data.

3.4.4 Nanosilica induces ASC expression in epithelial and endothelial cells

ASC (Apoptosis-associated Speck-like protein containing a CARD, caspase recruitment domain) was first discovered as it induced apoptosis in HL-60 leukemia cell lines when overexpressed [Masumoto *et al.*, 1999]. It is also called as TMS1 (Target of Methylation-mediated Silencing) and considered to be a tumor suppressor gene as its expression is downregulated by methylation of CpG islands in *Pycard* gene in different tumors such as breast cancer, glioblastoma and prostate cancer[Conway *et al.*, 2000; Das *et al.*, 2006; Stone *et al.*, 2004]. ASC acts as an adaptor protein in inflammatory pathways and helps in the assembly of supramolecular structures called inflammasome. ASC consists of a PYRIN domain and CARD domain, and it is localized in the perinuclear region of the cell [Srinivasula *et al.*, 2002]. It activates procaspase-1 into caspase-1. Caspase-1, in turn, acts on several different substrates involved in various pathways such as glycolysis, endotoxic shock, and activation of inflammatory cytokines such as IL-1β and IL-18[Shao *et al.*, 2007]. ASC also functions in an NLR independent manner by forming 1-2μm speck-like structure, also called 'pyroptosome'[Fernandes-Alnemri *et al.*, 2007]. ASC specks are also the sites for procaspase-1 recruitment and activation. ASC specks can also activate procaspase-8 and leads to apoptosis [Vajjhala *et al.*, 2015].

Silica nanoparticles of 12nm and 22nm showed increased expression of ASC protein in both epithelial and endothelial cell lines. The epithelial cell line showed higher ASC expression after the exposure of 12nm silica nanoparticles as compared to the 22nm silica nanoparticles (Figure 3.5)

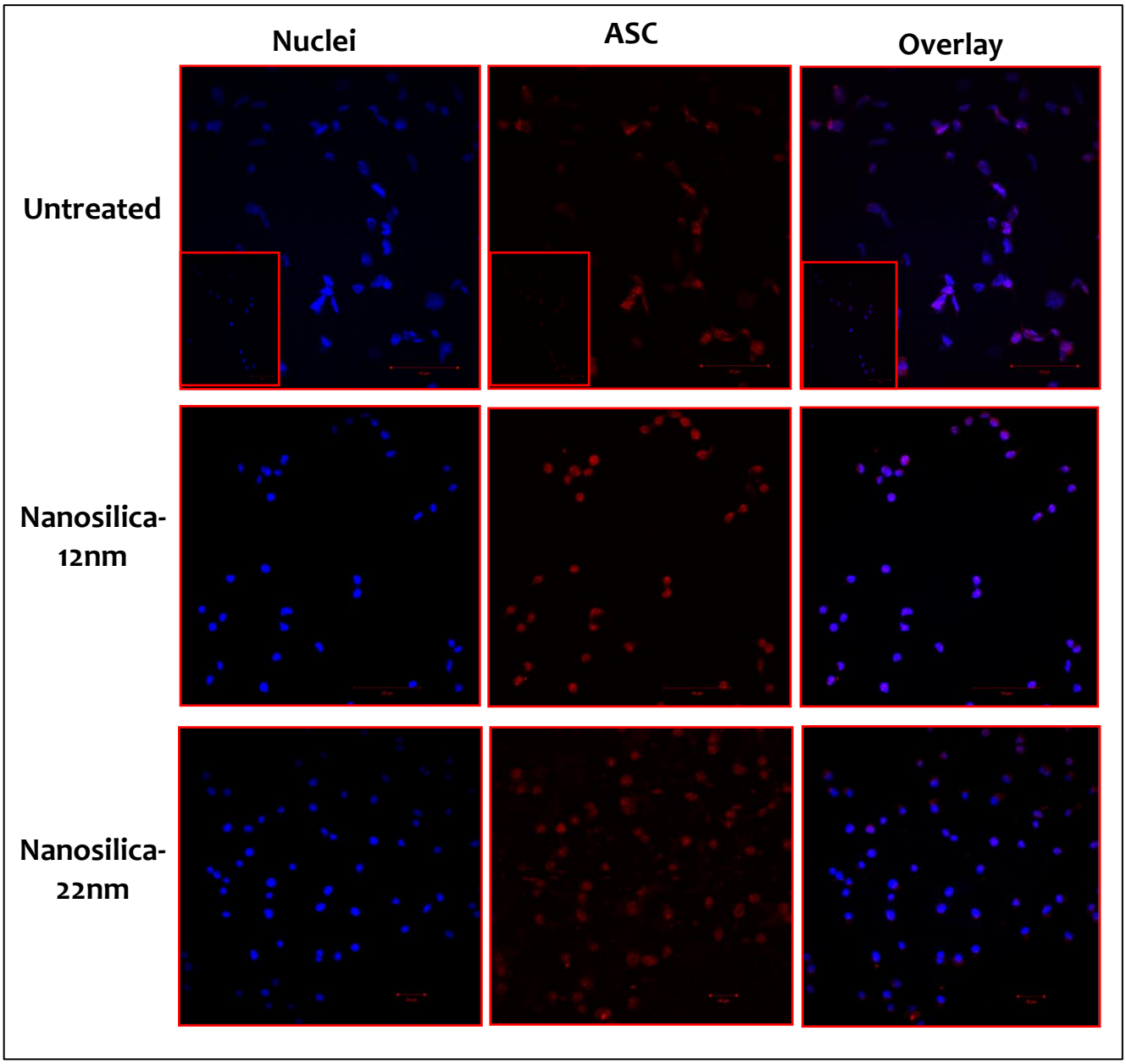

Figure 3.5: ASC expression was analyzed by immunofluorescence in epithelial cells. Anti-ASC antibody was used to stain ASC red. DAPI was used to stain nuclei blue. The untreated epithelial cells showed a diffused expression of ASC throughout the cell.

Endothelial cells were highly susceptible to nanosilica induced cell death also showed an ASC speck formation. While epithelial cells showed diffuse expression of ASC, endothelial cells had distinct ASC specks which were further quantified by confocal microscopy (Figure 3.6)

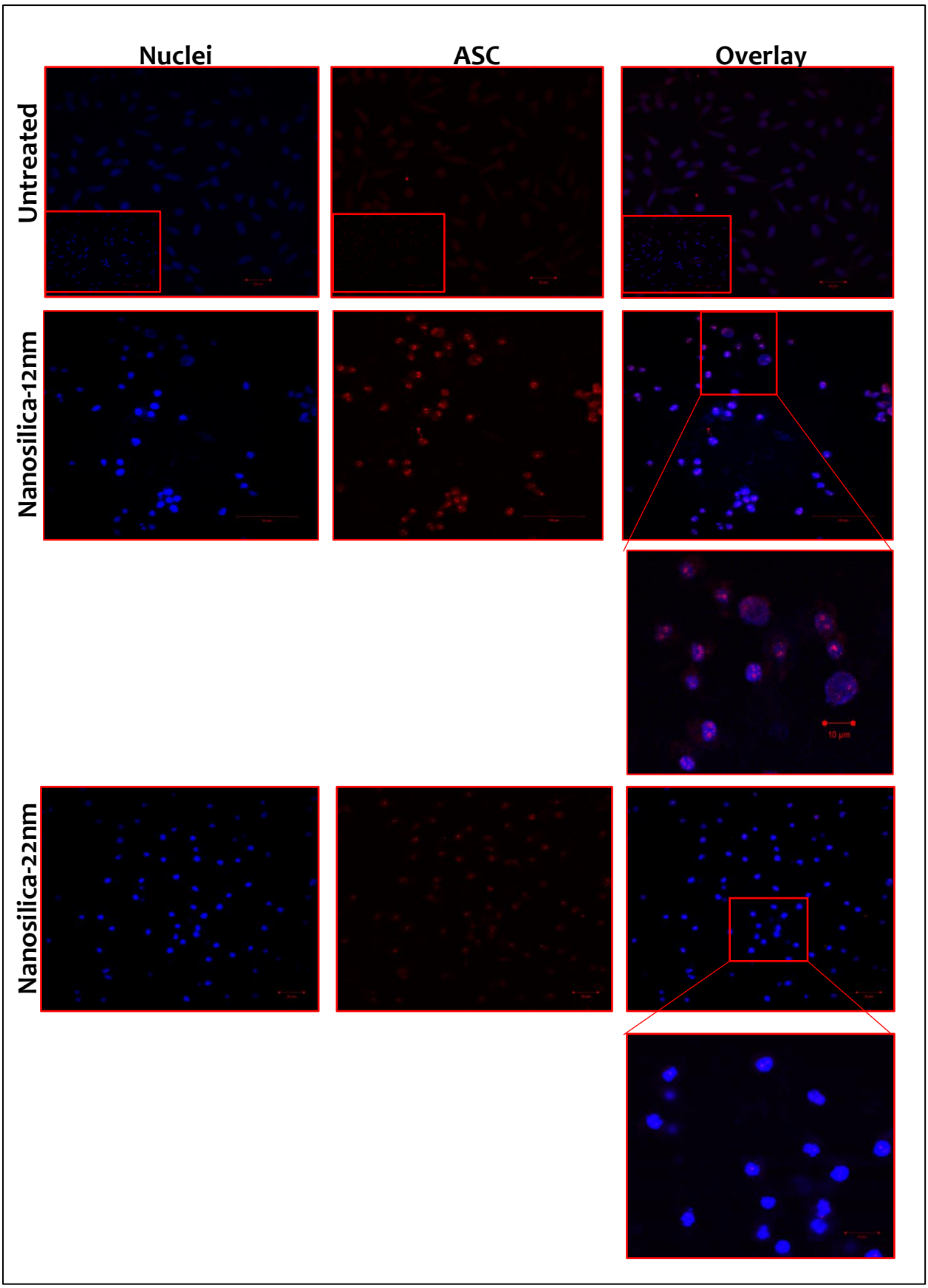

Figure 3.6: ASC expression was analysed by immunofluorescence in endothelial cells. Anti-ASC antibody was used to stain ASC red. DAPI was used to stain nuclei blue. The untreated epithelial cells showed a diffused expression of ASC throughout the cell; the antibody control showed (inset) no ASC expression. The 12nm and 22nm silica nanoparticles treated endothelial cells Scale bar is 20µm and 10µm

3.4.5 Nanosilica induces nuclear localization of ASC protein

Inactivated form of ASC is localized in cytoplasm or perinuclear space of the myeloid cells, and it gets activated in the presence of stimuli to form ASC speck or pyroptosome[Elliott and Sutterwala, 2015; Wang *et al.*, 2013]. On the contrary, Bryan et al. suggested that intracellular redistribution of the ASC from the nucleus to the cytoplasm is necessary for the activation of the functional ASC speck formation [Bryan *et al.*, 2009]. ASC is sequestered inside the nuclei in the resting macrophages and comes out to the cytoplasm or the perinuclear space once macrophages are activated in the presence of danger signals or cellular stress. 12nm and 22nm silica nanoparticles treated endothelial cells showed nuclear localization of ASC; this has been reported for the first time in this study. The 12nm silica nanoparticles treated endothelial cells showed nuclear localization of distinct ASC punctate structures along with perinuclear ASC specks (Figure 3.7). While the 22nm silica nanoparticles treated endothelial cells showed diffused ASC expression inside the nucleus. Confirmation of nuclear localization was done by z-stacking, which revealed the co-localization of fluorescence signals of anti-ASC antibody (red) and nuclear stain (DAPI, blue) (figure3.7).

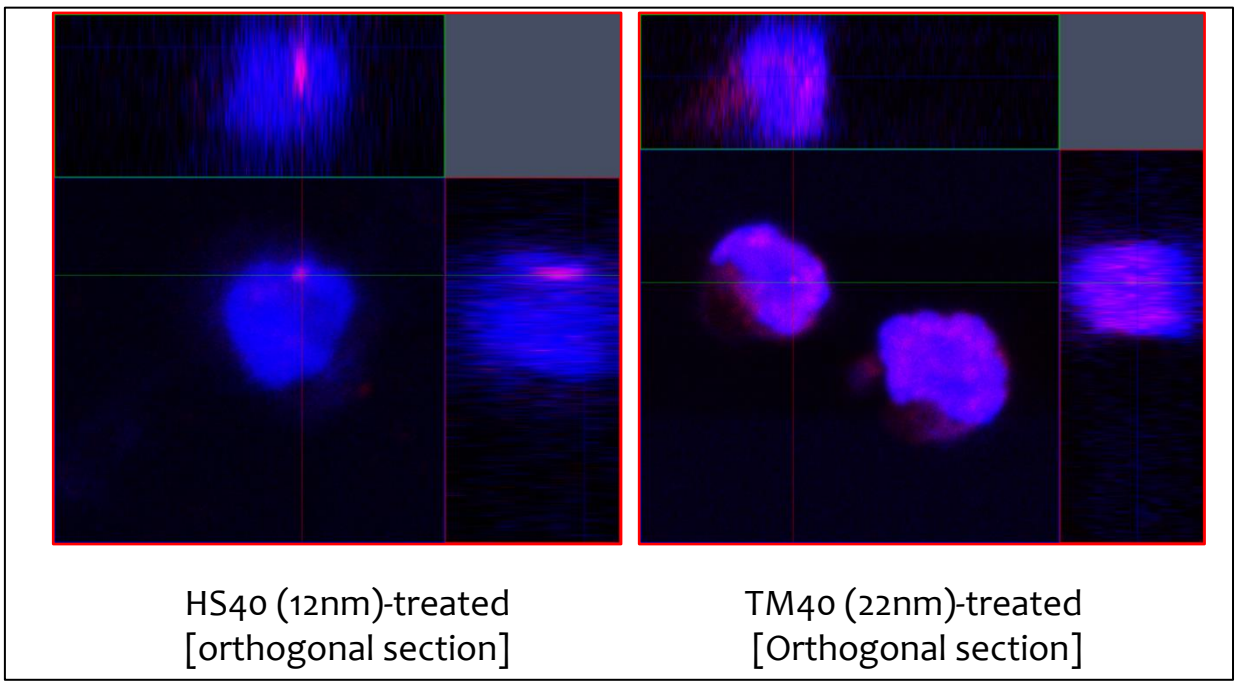

Figure3.7 Nuclear localization of ASC: Representative image showing orthogonal section confirming nuclear localization of ASC protein is within the endothelial cell.

Endothelial cells are more susceptible to silica nanoparticles induced cell death as compared to epithelial cells (previously confirmed by my colleagues). Endothelial cells also showed more expression of ASC as compared to epithelial cells (Figure 3.6 Quantification of ASC specks in the 12nm and 22nm silica nanoparticles treated endothelial cells was also performed by confocal microscopy. The 22nm silica nanoparticles treated endothelial cells have a significantly increased number of ASC specks as compared to the 12nm silica nanoparticles (Figure 3.8). Prior treatment of cytochalasin D with silica nanoparticles lead to decrease in the ASC speck count but did not cease it completely; which shows that phagocytosis might be involved as one of the pathways to engulf silica nanoparticles (Figure 3.8)

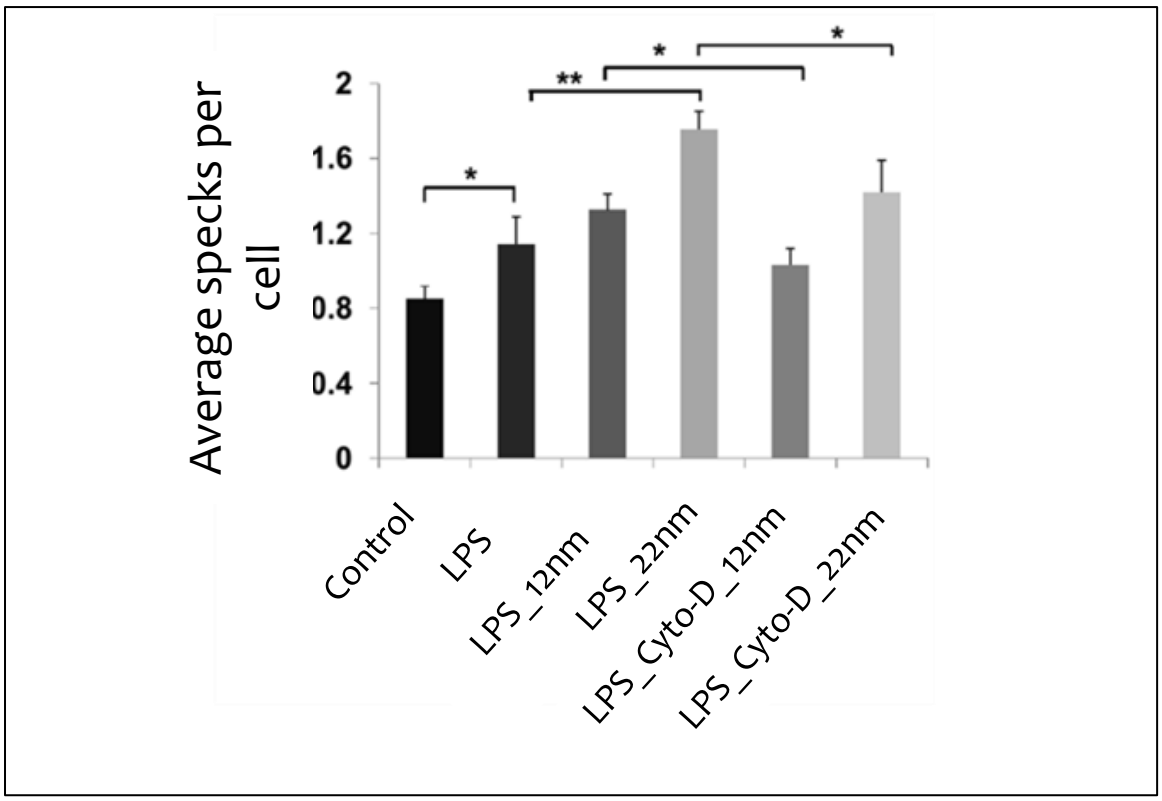

Figure 3.8: Quantification of ASC specks: ASC specks quantification in nanosilica treated endothelial cells. The graph represents number of specks/cell in untreated, nanosilica (HS40, TM40) and cytochalasin-D pretreated cells exposed to nanosilica (HS40, TM40). Data are represented as SEM (standard error mean). *$p < 0.05$, ** $p < 0.005$and ***$p < 0.0001$(Student's t-test).

3.4.6 12nm and 22nm silica nanoparticles induced distinct cell death pathways

ASC speck formation has been linked with pyroptosis, which is a caspase-1 mediated cell death. ASC speck formation has also been linked to caspase-1 independent cell death, i.e., apoptosis. Apoptosis is described as programmed cell death in which the cell undergoes morphological changes such as nuclear fragmentation, cell shrinkage, chromosome condensation and plasma membrane blebbing [Zhang *et al.*, 2017]. ASC has been reported to induce both pyroptosis and apoptosis in case of bone marrow-derived macrophages (BMMs) transfected with DNA [Sagulenko *et al.*, 2013]. The lower concentration of transfected DNA led to apoptosis while higher DNA concentration induced pyroptosis. ASC pyrin domain nucleates procaspase-8 death effector domain (DED) filaments to induce apoptosis in cells with activated inflammasomes [Vajjhala *et al.*, 2015].

The 12nm and 22nm silica nanoparticles induced cell death was observed by transmission electron microscopy image courtesy Dr. Nidhi Sharma and Dr. Radhika Poojari. The 22nm silica nanoparticles showed characteristics features of apoptosis while 12nm silica nanoparticles induce necrosis with loss of membrane integrity, intracellular organelle, and cytoplasm swelling (Figure 3.9a). To quantify the nature of cell death, Annexin V-propidium iodide staining was performed. Annexin V binds to the phosphatidylserine which comes out on the surface from the inner side of the plasma membrane. Propidium iodide is permeable to necrotic cells but does not enter apoptotic cells [Crowley *et al.*, 2016]. The viable cells are both Propidium iodide and Annexin V negative, which consists of 86% untreated cells. In case of 12nm silica nanoparticles treated cells 81.7% cells were necrotic cells (PI-positive); while 22nm silica nanoparticles treated cells were apoptotic (33.4% Annexin V positive cells, 58% double-positive cells)(Figure 3.9b).

3.9 a

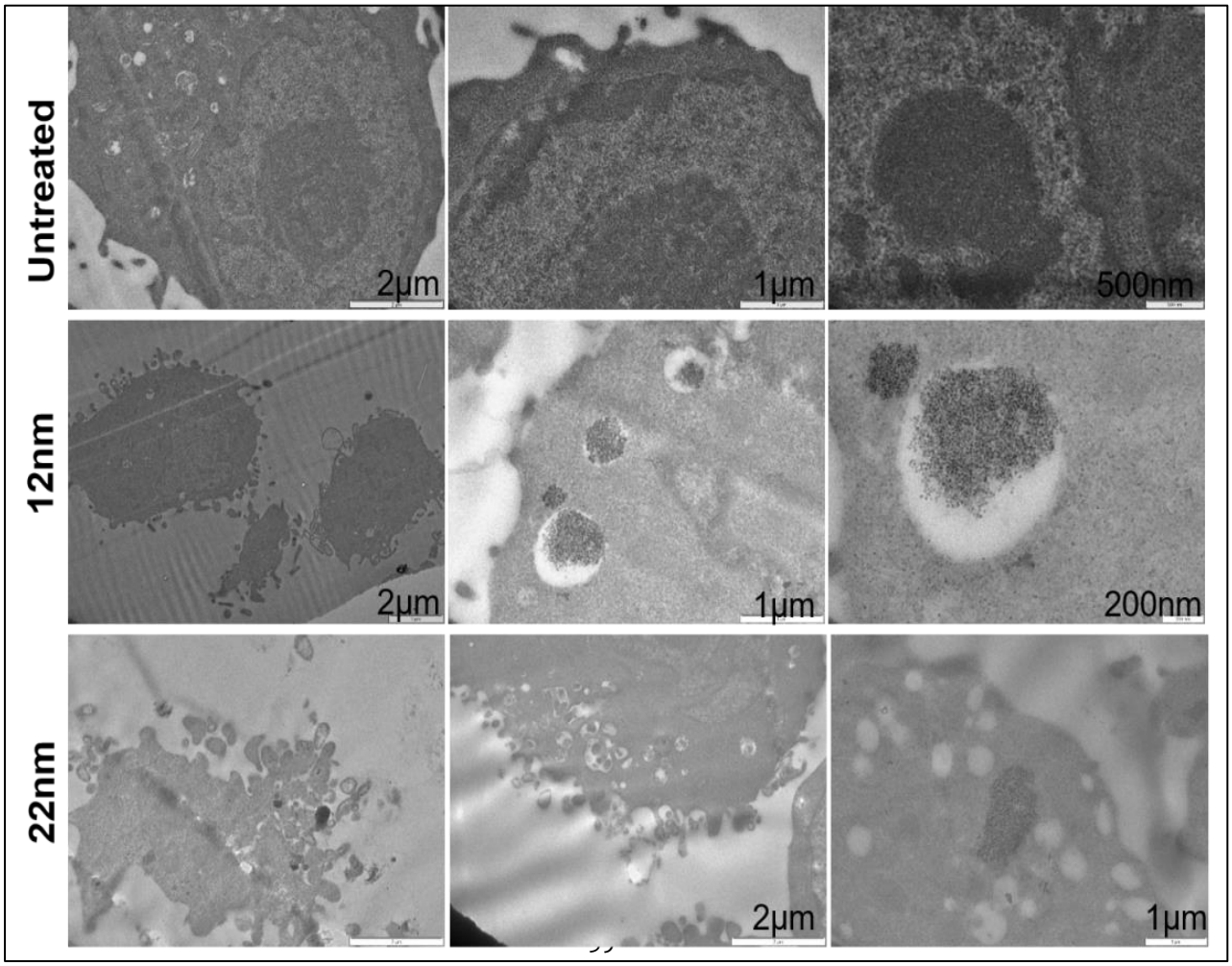

3.9 b

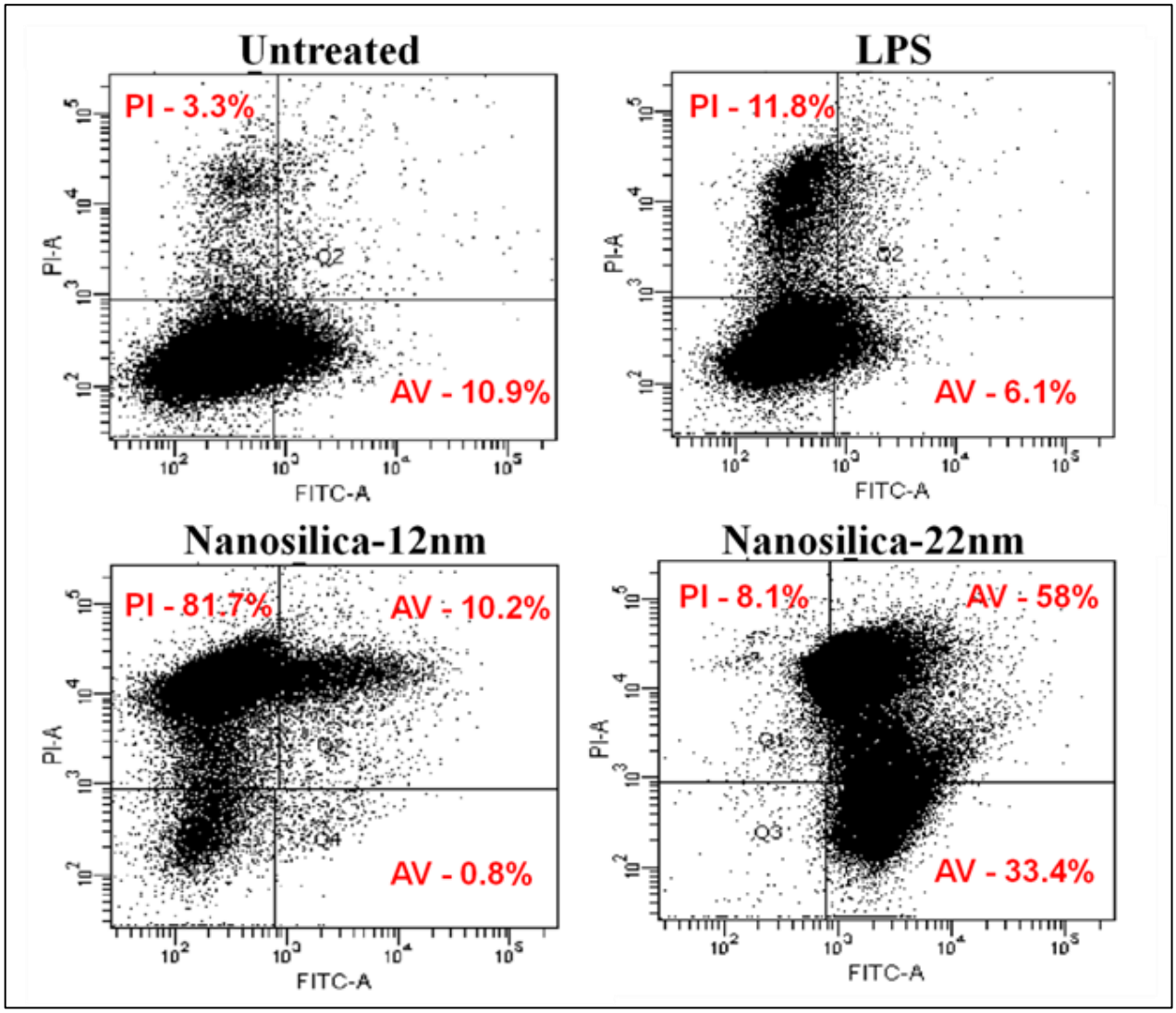

Figure 3.9: Characterization of internalization of nanosilica and subsequent cell death. Transmission electron microscopy of 12nm treated cells show characteristic necrotic morphology while 22nm treated cells appear apoptotic (a). Flow cytometry for cell death phenotype analysis by Annexin V-PI staining (b). Approximately 86% of untreated cells and LPS treated cells are Annexin V and PI negative. In case of 12nm nanosilica treated cells, 81.7% cells are PI positive, 0.8% cells are Annexin V positive and 10.2% cells are AnnexinV/PI double positive. In contrast 22nm nanosilica treated cells show 33.4% Annexin V positive cells, 58% double positive cells and 8.1% PI positive cells.

3.4.7 Nanosilica induces caspase-1 independent cell death in microglial cells

Caspase-1 activation plays a central role in the NLRP3 mediated inflammatory pathway. Crystalline silica activates NLRP3 inflammasome, which cleaves caspase-1[Cassel *et al.*, 2008]. To investigate whether caspase- 1 plays a role in amorphous nano silica-induced cell death, we measured the active caspase-1 activity by the cleavage of a fluorescent caspase-1 substrate (Ac-WEHD-amc). The caspase-1 substrate show has an excitation maximum of 340-360nm and an emission maximum of 440-460nm. We measured the fluorescent activity of the substrate by immunofluorescence as well as protein assay. We

observed no change in the fluorescent activity of caspase-1 substrate between the control and the nanosilica treated cells (Figure 3.10 a and 3.10 b)

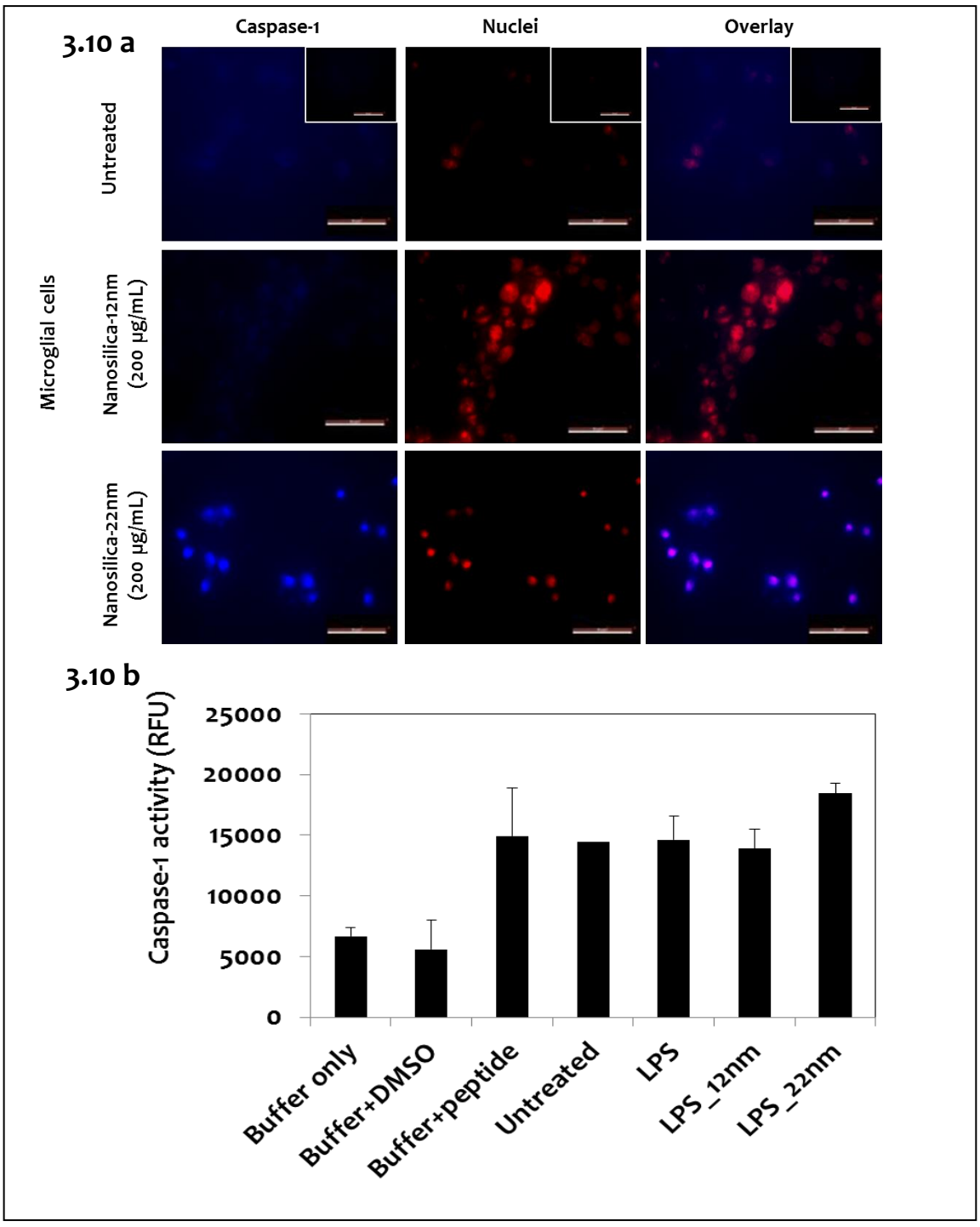

Figure 3.10 Activated caspase-1 expression in nanosilica treated microglial cells. a) Fluorescent caspase-1 substrate (Ac-WEHD-amc) was used to stain caspase-1 (blue). Propidium iodide (PI) was used to stain nuclei (red). Untreated, 12nm and 22nm nanosilica treated microglial cells were stained for caspase-1 and PI. In 22nm nanosilica treated cells, caspase-1 expression increased as compared to 12nm nanosilica treated microglial cells. Here, inset shows PI control. Scale bar: 50µm. b) Caspase-1 activation in nanosilica treated microglial cells. To simulate inflammation, microglial cells (BV-2) were primed overnight with LPS (0.5µg/mL) before exposure to both 12 and 22nm nanosilica particles (200µg/mL; 60 minutes).Error bars indicate standard error of mean (SEM). Relative fluorescence unit (RFU) n=2

3.5 Concluding remarks

Nanoparticles have an ever-increasing role in various fields such as pharmaceuticals, bio-pesticides, cosmetics, and electronics. There are divided opinions about whether the silica nanoparticles are inert or their constant exposure can cause respiratory diseases. In 2010, Yazdi et al. investigated the inflammatory effects of nanoparticles and concluded that both titanium and silica nanoparticles (30nm) induced IL-1β secretion in a dose s dependent manner [Yazdi *et al.*, 2010]. Silica nanoparticles (70nm) injected intravenous has also been shown to restrict the growth of the fetus in mice. Although the modifications of the surface with amine and carboxyl group reduced the negative effects on the pregnant mice [Yamashita *et al.*, 2011]. In case of atopic dermatitis as well the deleterious effects of silica nanoparticles (30nm) were confirmed in the form of increased inflammation and release of cytokines such as IL-18 and thymic stromal lymphopoietin(TSLP)[Hirai *et al.*, 2012]. Increase in inflammation leads to systemic Th2 response. Most of the studies done so far are focused on the silica nanoparticles sized more than 30nm. I have studied the nanoparticles sized 12nm and 22nm, which also takes into consideration that smaller silica nanoparticles have higher surface energy. Exposure of silica nanoparticles has led to the endothelial cell death in a concentration-dependent manner. Cytochalasin D, an inhibitor of actin polymerization, has been shown to inhibit internalization of silica nanoparticles sized 30nm or more [Kusaka *et al.*, 2014]. This actin-cytoskeleton-dependent phagocytosis inhibition led to the decreased cell death in the larger silica nanoparticles while the smaller silica nanoparticles showed no effect of cytochalasin D on cell death.

ASC, an adaptor protein, expression increased in the silica nanoparticles treated endothelial cells. Differential ASC expression was observed in case of larger silica nanoparticles treated endothelial cells as compared to smaller silica nanoparticles. The smaller silica nanoparticles treated endothelial cells have shown to have a functional speck formation while larger silica nanoparticles treated endothelial cells have diffused ASC expression. During the study, we observed for the first time to our knowledge that ASC expression following silica nanoparticles treatment to be localized inside the nucleus, which was confirmed by confocal microscopy. I further confirmed the nature of cell death in the silica nanoparticles treated cells, which was also different in different nanosilica. The larger silica nanoparticles treated cells had apoptotic cell death, and smaller silica nanoparticles treated cells had necrotic cell death. This study confirms that silica nanoparticles induced inflammation can be cytotoxic. Even though 22nm silica nanoparticles can be internalized by macrophages, they will eventually be realized by dying marcophages. The 12nm silica nanoparticles have the danger of being directly internalized by the exposed cells. Further inflammatory and toxicokinetics can be performed to analyze the health effects of these silica nanoparticles. With this study, we suggest a precautionary statement for the widespread usage of the silica nanoparticles.